S.Moser, M.Ivanisin, J.Woisetschläger, H.Jericha (2000) *Novel Blade Cooling Engineering Solution*, ASME International Gas Turbine and Aeroengine Congress, Munich, 2000-GT-0242

NOVEL BLADE COOLING ENGINEERING SOLUTION

Siegfried Moser, Mario Ivanisin, Jakob Woisetschläger, Herbert Jericha
Institute for Thermal Turbomachinery and Machine Dynamics
Technical University Graz
Inffeldgasse 25
A-8010 Graz / Austria

ABSTRACT

The evolution of increasing turbine inlet temperature has led to the necessity of full-coverage film cooling for the first turbine vane and blade. In this paper a new approach using transonic wall film jets for blade and vane cooling is investigated to provide a first guideline for engineering design. The first part presents a Computation Fluid Dynamics (CFD) cooling efficiency investigation on a flat plate with varied injection angles and blowing ratios. With these results detailed 2D- and 3D-Navier-Stokes external flow calculations coupled with the appropriate solid heat conduction calculations for a cooled turbine blade were modelled. On the basis of heat transfer and temperature distribution of the blade a Finite Element Analysis (FEA) was realised.

NOMENCLATURE

BR	blowing ratio = $(\rho_c v_c)/(\rho_g v_g)$
c	blade chord length [mm]
d	blade height [mm]
DR	density ratio = $(\rho_c/(\rho_g)$
h	slit height [mm]
IR	momentum flux ratio = $(\rho_c v_c^2)/(\rho_g v_g^2)$
k	turbulent kinetic energy [m^2/s^2]
M	Mach number
m	mass flow [kg/s]
MR	mass flux ratio = (m_c/m_g)
p	pressure [bar]
Q	heat flux [W/m^2]
T	temperature [K]
Tu	turbulence intensity [%]
x	chordwise coordinate [m]

Greek

α	heat transfer coefficient = $q/(T_{wall}-T_{\infty\ tot})$ [W/m^2K]
β	injection angle of slits
η	film cooling effectiveness
ρ	density [kg/m^3]

Indices

ad	adiabatic
aw	adiabatic wall condition
c	coolant flow
∞	main flow condition
r	recovery
tot	total condition
w2	adiabatic cooled wall condition
wall	wall condition

INTRODUCTION

One way to improve efficiency in modern gas turbines is to increase the turbine inlet temperature. Additionally, modern turbines are designed for increasing mass stream and pressure ratio in the turbine stages leading to transonic conditions in these machines. These conditions cause pronounced shock systems interfering with the cooling films covering the blade surfaces.

Therefore, an improved cooling system not only has to have high cooling effectiveness thus keeping the increased blade temperature distribution at uniform level to ensure high reliability and prolong the thermal fatigue life. It also has to have high resistance against free stream turbulence and shock waves in transonic gas turbines.

The innovative cooling system developed at the Institute for Thermal Turbomachinery and Machine Dynamics at Technical University Graz promises several new features in meeting the objectives.

Originally, this cooling system was intended for industrial steam-injected gas turbine for cogeneration systems where steam at low temperature and high pressure is available (Jericha et al., 1995), (Satoh et al., 1991), (Ishizuka et al., 1991), but the application to a gas turbine cycle using air as cooling medium is under discussion.

The characteristic of this cooling method proposed is a cooling film making use of the behaviour of under expanded jets. An under

expanded jet means a jet from a choked convergent nozzle where the flow subsequently expands supersonically because the external pressure is below the critical value. These jets have a strong tendency to bend towards a convex surface what was shown by Gilchrist and Gregory-Smith., (1988), Gregory-Smith and Gilchrist., (1987), and Gregory-Smith and Hawkins, (1991). This effect is called Prandtl-Meyer-Effect.

In the cause of gas turbine development work a favourable application of under expanded films for gas turbine blade cooling was envisaged by Jericha et al. (1997). Earlier experimental investigations of Woisetschläger et al. (1995, 1997), Gehrer et al. (1997) and Moser et al. (1999) with this type of cooling film in the leading edge area showed a coolant film coherently covering the surface with a strong adherence to it. The influence of strong upstream flow distortions especially in the leading edge area have been tested by Moser et al. (1998). Consequently the cooling efficiency and heat transfer behavior had to be investigated. The present work presents an engineering solution of the cooling method.

INVESTIGATION OF COOLING EFFICIENCY ON A FLAT PLATE USING COMPUTATION FLUID DYNAMICS

A numerical study had been conducted to investigate the effects of turbulence, mainflow velocity, cooling slit height and angle of cooling flow injection to the cooling efficiency on a flat plate. For these calculations a commercial Navier-Stokes code (Fluent 5.1, Fluent Inc.) has been used.

Theoretical Background

The following definitions and equations were chosen in accordance with the definitions given by Goldstein (1971). The adiabatic film cooling effectiveness, η_{ad}, is defined according to the following equation:

$$\eta_{ad} = \frac{T_{aw} - T_\infty}{T_c - T_\infty} \qquad (1)$$

This is the equation for low speed, constant property flow, where the cooling fluid temperature T_c and the main stream temperature T_{oo} are assumed constant. Note that in a film cooling application in general for the wall temperature T_{aw} and the cooling fluid temperature T_c. the following relation is valid:

$$T_{aw} < T_\infty \text{ and } T_c < T_\infty$$

Also note that the film cooling effectiveness usually varies from unity at the point of injection (where the wall temperature on the plate T_{aw} equals cooling fluid temperature T_c to zero far downstream. There, the adiabatic wall temperature T_{aw} approaches the main stream temperature T_∞, because of the mixing of the main flow with the cooling flow (assumption of low speed, incompressible flow).

For high-speed flows the film cooling effectiveness must be defined somewhat differently. At the point of injection, the cooling slit exit wall-temperature T_{w2} is the recovery temperature of the cooling flow, which is slightly less than the total temperature T_c of the cooling flow. Far downstream on the plate, the wall temperature T_{aw} will approach the main stream recovery temperature T_r, which is slightly less than the total temperature T_∞ of the main flow. An expression used by Goldstein (1971) for compressible flow film cooling is

$$\eta_{ad} = \frac{T_{aw} - T_r}{T_{w2} - T_r} \qquad (2)$$

Note that the film cooling effectiveness η_{ad} reduces to equation (1) when compressiblity effects can be neglected.

In the case of underexpanded cooling jets we found that the cooling slit exit wall-temperature T_{w2} depends not only on the pressure ratio between main flow and cooling flow but also on the cooling slit height. It means that with equal main flow and cooling flow conditions T_{w2} decreases. This effect leads to unwanted falsifications of the efficiency For that reason the following definition for "adiabatic film cooling effectiveness" η_{ad} according to total cooling Temperature was used:

$$\eta_{ad} = \frac{T_{aw} - T_r}{T_c - T_r} \qquad (3)$$

where T_c is the total temperature of the cooling fluid. Here, the cooling effectiveness may vary from more than unity at the point of injection to zero far downstream. In this way a serious comparison of the efficiency with varying boundary conditions is possible.

Computational grids

Structured 2D-multiblock hybrid grids were used to discretize the flow region (s. Figs. 1 and 2) throughout this paper. These grids allow a resolving the boundary layers down to the viscous sub-layer.

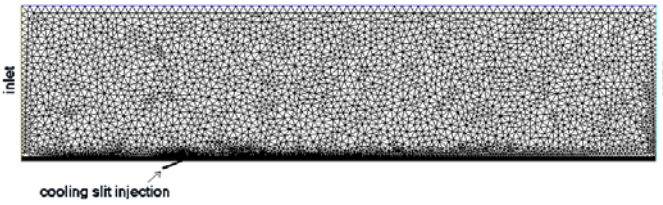

Fig.1: Computional hybrid grid of flat plate with cooling slit

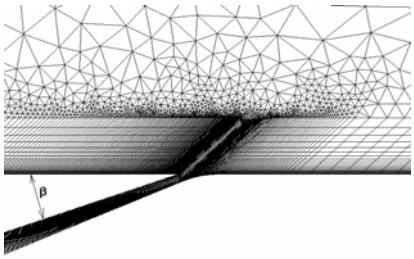

Fig.2: Zoomed computational grid at slit area

Solver

The compressible coupled time–marching implicit solver implemented in Fluent 5.1 was used for the calculations.

Turbulence model

The turbulence of the flow was modelled with a two-equation standard k-epsilon model combined with a two layer zonal model of Wolfstein (1969) for resolving the boundary layers.∞

Boundary conditions

For the following parameter study differently parameter were varied. On the one hand flow conditions were changed on the other hand the slit outlet height was modified from 0,2 mm to 0,4 mm . In the table 1 the boundary conditions are summarized. These data are to be linked then direct with the solutions in the Figs. 3 to 6.

Table 1: Flow conditions

mainflow	see Fig. 3	see Fig. 4	see Fig. 5	see Fig. 6
$T_{\infty\ tot}$ [K]	323	323	323	323
$p_{\infty\ tot}$ [bar]	1.3	1.3, 1.07	1.3, 1.07	1.3, 1.07
$p_{\infty\ stat}$ [bar]	1	1	1	1
Tu_∞ [%]	1	1, 10	1, 10	1
M, isen.	0.6	0.3, 0.6	0.3, 0.6	0.6
gas	air			
coolant flow				
h [mm]	0.4	0.4	0.2	0.2, 0.4
β [°]	20, 30, 40	20	20 °	20 °
$T_{c\ tot}$ [K]	298	298	298	298
$p_{c\ tot}$ [bar]	2	2	2	2
BR	1.86	1.86, 3.81	1.86, 3.81	1.86
DR	1.23	1.23, 1.30	1.23, 1.30	1.23
IR	2.81	2.81, 11.22	2.81, 11.22	2.81
Tu_c [%]	10	1	1	1
injection gas	air			

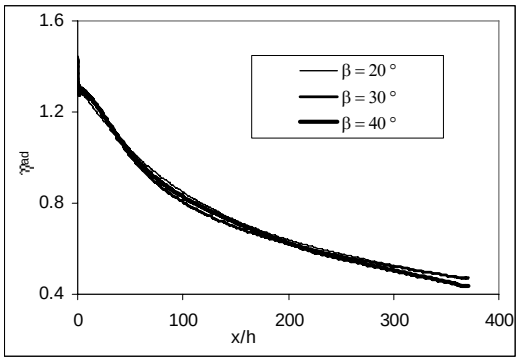

Fig.3: Comparison of adiabatic cooling efficiency for different cooling inflow angles β

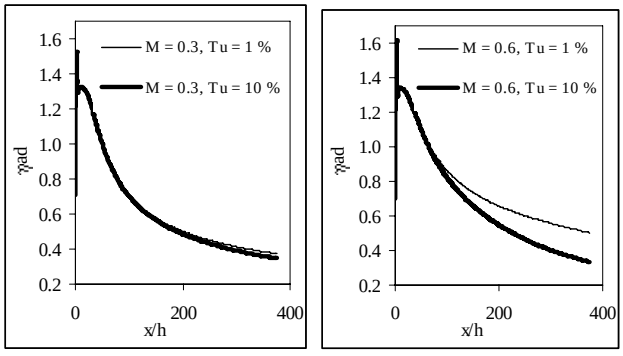

Fig. 4: Comparison of adiabatic cooling efficiency for different mainflow Mach numbers and mainflow turbulence intensities for a cooling slit height of h = 0.4 mm (see Table 1)

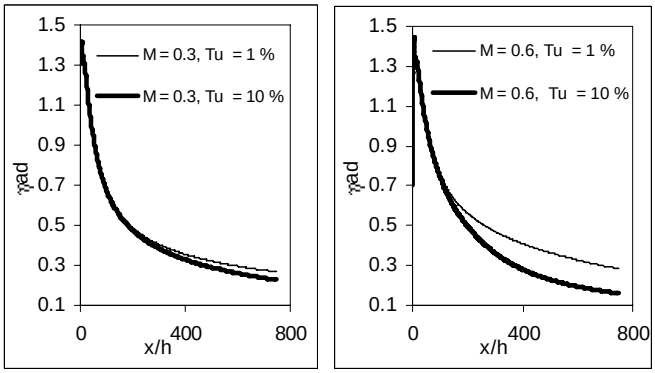

Fig. 5: Comparison of adiabatic cooling efficiency for different mainflow Mach numbers and mainflow turbulence intensities for a cooling slit height of h = 0.2 mm (see Table 1)

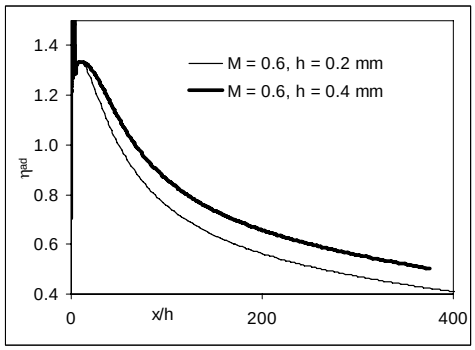

Fig. 6: Comparison of adiabatic cooling efficiency for equal flow conditions but different slit heights (see Table 1)

Results and discussion

For the under expanded cooling film the influence of the slit inflow angle β (varied from 20° to 40°) to the cooling efficiency is negligible (see Fig. 3). That is to be attributed to the fact that the jet also with large angle do not lift off at slit outlet area due to the Prandl-Meyer-Effect.

The influence of the turbulence intensity of mainflow on η_{ad} is depicted in Fig. 4 and Fig. 5 for different Mach numbers and slit heights. For a Mach number of 0.6, η_{ad} is lower for the hight turbulence case due to stronger mixing in the boundary layer. This effect is independent of the slot height (compare Fig. 4 and Fig. 5). It is interesting that with smaller Mach numbers the efficiency is hardly influenced by the turbulence. A possible assertion is that the turbulent kinetic Energy of the mainflow with rising Mach number rises with a square function (see Table 2). That leads to the assumption that the ”destruction strength” of the mainflow depends on the turbulent kinetic energy. From this it can be derived that the turbulent kinetic energy is more efficient size for the evaluation of cooling jets than the turbulence intensity.

Table 2 Comparison of turbulence Intensities and turbulent kinetic energies in dependency of the Mach numbers

M, isen.	0.3	0.3	0.6	0.6
Tu_∞ [%]	1	10	10,	10
k [m^2/s^2]	≈ 1.8	≈ 180	≈ 6.7	≈ 664

A slit height enlargement from h = 0.2 mm to 0.4 mm increases the efficiency by approx. 10 % at x/h = 350 (see Fig. 6).

Further the calculations showed that there is almost no influence of the cool flow turbulence intensity Tu_c on the cooling efficiency what isn't presented here (compare Fig. 3 with Fig5).

Table 2 Comparison of turbulence Intensities and turbulent kinetic energies in dependency of the Mach numbers

INVESTIGATION OF TURBINE BLADE USING 2-DIMENSIONAL COMPUTATIONAL FLUID DYNAMICS

Geometry

A cross sectional view of the investigated blade design with cooling slits is given in Fig 7. In Table 3 all characteristic data of the blade are summarized.

The slit arrangement took place after detailed experimental and numerical investigations. Special attention was put on slit #2. The jet at this slit has the function to cool the highly stressed leading edge by covering it completely with a cooling film by bending around these. Besides the jet must be resistant to pressure waves and/or flow disturbances caused from the nozzle trailing edge.

Slit #1 is positioned as near as possible at slot #2, so that the intermediate surface is cooled sufficiently from the inside due conduction. Slot #3 should attach where the jet of slot #2 its effect loses. The same applies to slot #4 and slot #5, which besides protect the leading edge against overheating.

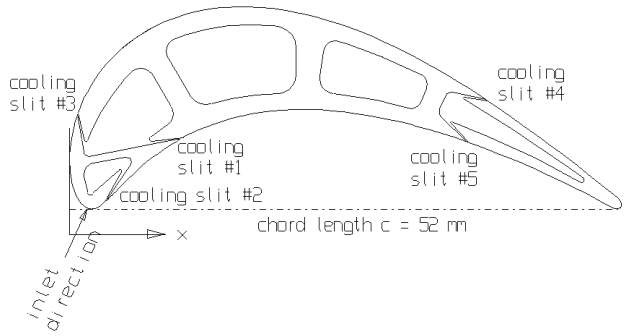

Fig. 7: Geometry of the blade with the position of the cooling slits

Table 3: Blade and cooling slit geometry

blade chord length	71 mm
blade height	26 mm
pitch/chord ratio	0.694
inlet angle*	55 °
outlet angle*	28 °
cooling slit length	6 mm
cooling slit height	0.2 mm
Position / angle to surface of slit #1	x/c = 10.5 / 22°
Position / angle to surface of slit #2	x/c = 10.5 / 11°
Position / angle to surface of slit #3	x/c = 10.5 / 27°
Position / angle to surface of slit #4	x/c = 10.5 / 23°
Position / angle to surface of slit #5	x/c = 10.5 / 25°

*measured from circumferential direction

Computational grids

Hybrid multiblock grids were used to discretize the flow region (see Fig. 8). For resolving the boundary layers down to the viscous sub-layer at blade and slit surfaces structured blocks were used (Fig. 9). For the solid and main flow parts an unstructered mesh was generated.

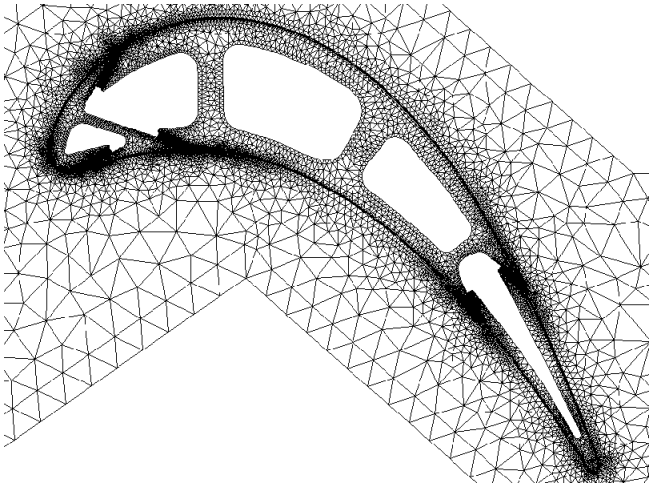

Fig. 8: Computional hybrid grid with cooling slits

With this grid y^+ values of smaller 4 at the coupling wall interfaces could be carried out. Figure 9. shows the grid refinement at the wall or at the slit #2 area.

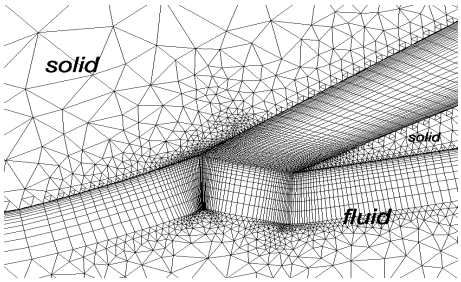

Fig. 9: Computational zoomed grid at slit #2 outlet area

Solver and Turbulence Model

Again, the compressible coupled time–marching implicit solver implemented in Fluent 5.1 was used for the calculations. The turbulence of the flow was modelled with a two-equation standard k-ε model combined with a two layer zonal model of Wolfstein (1969) for resolving the boundary layers. The standard k-ε model has become an useful tool for general technical engineering solutions since it was proposed by Jones and Launder (1972). The k-e model is a semi-empirical model based on model transport equations for the turbulent kinetic energy (k) and its dissipation rate (ε). The model transport equation for k is derived from the exact equation, while the model transport equation for ε was obtained using physical reasoning. In the derivation of the k-ε model, it was assumed that the flow is fully turbulent, and the effects of molecular viscosity are negligible. The standard k-ε model is therefore valid only for fully turbulent flows.

Boundary conditions

The boundary conditions (see Table 4) of the mainflow were selected in such a way, so that the Reynolds numbers and turbulence intensities correspond to a real gas turbine. The inlet velocity profile was assumed constant. The constant total inlet temperature of 1673 K was very highly assumed.

The interior of the blade is devided into five cooling channels, through which the separating walls act as cooling ribs for the outer surface. The walls of the blade have constant thickness and the internal cooling boundary conditions (see Table5 and Table 6) are fixed to constant values, thus providing a constant cooling potential on all internal surfaces. The cooling air temperatur of 773 K compares to exit temperatures of today's compressor and the internal heat transfer of 550 W/m^2K is a typical value for enhanced ribbed cooling channel heat transfer. The high cooling fluid total pressure of over 30 bar is achieved either with the help of an additional compressor or as mentioned in the introduction with steam from a cogeneration system where steam at low temperature and high pressure is available.

As material a usual turbine steel was selected (see Table 7).

Table 4: Mainflow conditions

mainflow	**inlet**	**outlet**
$T_{\infty\ tot}$ [K]	1673	
$p_{\infty\ tot}$ [bar]	15	
$p_{\infty\ stat}$ [bar]		8.87
Tu_{∞} [%]	10	
Re	$6.215 \cdot 10^5$	$1.443 \cdot 10^6$
M, isentropic	0.29	0.90
gas	air	

Table 5: Cooling jet conditions

coolant flow	**inlet**
$T_{c\ tot}$ [K]	773
$p_{c\ tot}$ [bar]	30
Tu_c [%]	10
MR	0.03
BR	3.09
injection gas	air

Table 6: Internal cooling channel conditions

$T_{c\ tot}$ [K]	773
α [W/m^2K]	550

Table7: Material data L326 VMR

Modulus of elasticity at 1173K	150000 N/mm^2
Specific heat capacity	460 J/kgK
Thermal conductivity at 1173 K	26 W/mK
Density	8220 kg/m^3
Mean coeff. of therm. Exp. at 1073 K	$15 \cdot 10^{-6}$ m/mK

Results of the 2-Dimensional Flow Analysis

A contour plot of the temperature distribution in the mainflow, the cooling flow and the solid part is shown in Fig. 10 and 11. Temperature and heat transfer distribution on the solid blade at suction and pressure side are presented in Figs. 12 to 15.

This 2-dimensional investigation served as pre-study to the following 3-dimensional calculations. Special care had been taken to achieve a uniform temperature distribution around the blade, especially at the leading edge pressure side. Here, two cooling film were ejected in opposite directions (slit 1 and 2 in Fig.13). This slit arrangement allowed an optimum cooling of the leading edge even under main flow pressure fluctuations up to 25% of $p_{\infty\ tot}$ what has been showed by Moser et al (1998).

Fig.:10: Temperature field [K]

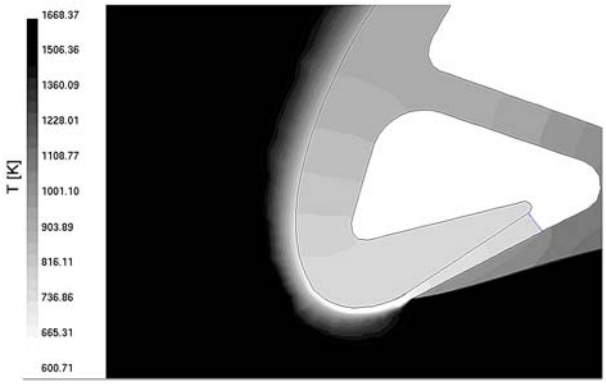

Fig.: 11: Temperature distribution [K] at leading edge area

Figure 12 shows the temperature increase at the nose and at the suction face, beginning with slot #2. At the leading edge it comes to a temperature peak of approx. 950 K. In the further the temperature due to the internal conductive cooling of the slot 3 decrease to approximate 900 K. At slot #3 it comes to a temperature branch on approx. 750 K due to the low under expanded cool flow temperature. The wall temperature at suction side increases to 1000 K. Slit #4 causes again an internal conductive cooling to 875 K. At the position of slit outlet the calculation shows again a branch of the wall temperature to about 750 K. The trailing edge temperature rises from 500 to 700 K.

A similar temperature behavior shows the pressure side of the blade (see Fig. 13). Here it must be paid attention to the distance between slit #1 and #2 because this surface isn't covered with a cooled film. Figure 13 shows a temperature peak of 1100 K what is in a tolerably range.

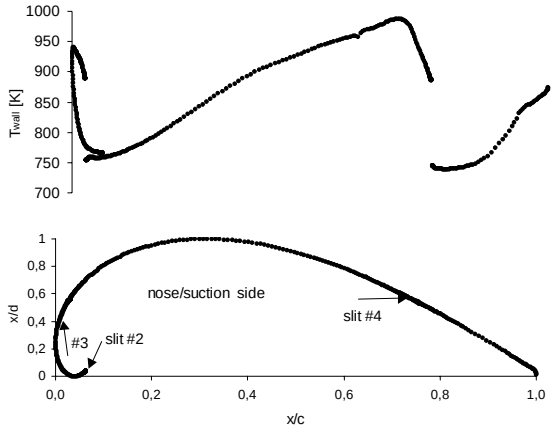

Fig.:12: Temperature distribution at nose- suction area

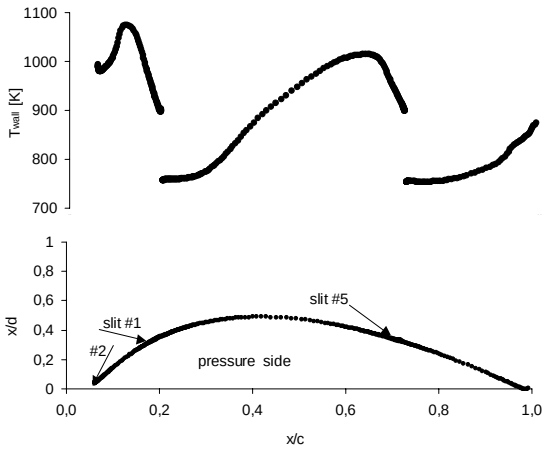

Fig.13: Temperature distribution pressure side

The heat transfer distribution at the blade are represented in Fig. 14 and Fig. 15. The surface heat transfer coefficient α is defined by the equation $\alpha = q/(T_{wall}-T_{\infty\ tot})$.

The negative heat transfer coefficients are remarkable. This effect is caused by the change of the heat flux direction. Because the low cooling flow outlet temperatures leads to low wall temperatures at the slit areas. That means that the internal channel is "cooled". Therefor the unsteadiness points of the heat transfer coefficients are located at the cooling slit outlets.

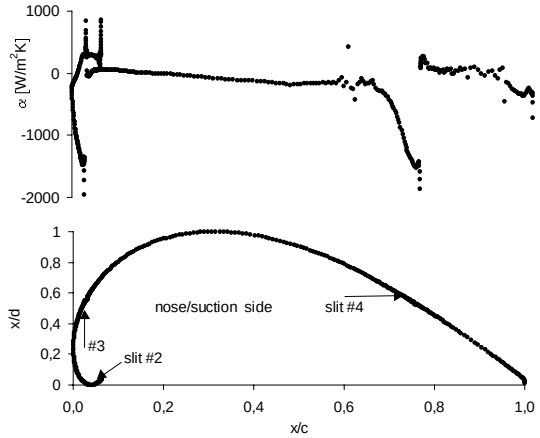

Fig. 14: Heat transfer coefficient distribution at leading edge – suction area

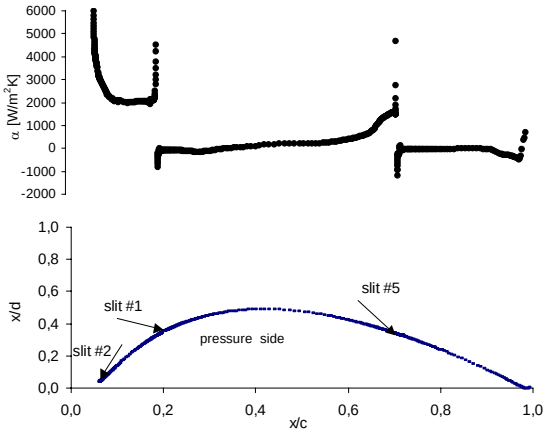

Fig. 15: Heat transfer coefficient distribution on pressure side

INVESTIGATION OF TURBINE BLADE USING 3-DIMENSIONAL COMPUTATIONAL FLUID DYNAMICS

The following 3-dimensional investigations had been performed with the solver and boundary conditions as the 2-dimensional calculations above.

Computational grids

In Fig. 16 and Fig. 17 the solid part of the 3-D grids are presented. The slits are located at the same positions as with the preceeding 2D-calculation. Instead of the two-zonal turbulence model the logarithmic wall function had been applied, which is implemented in FLUENT 5.1. based on the proposal of Launder and Spalding (1974).

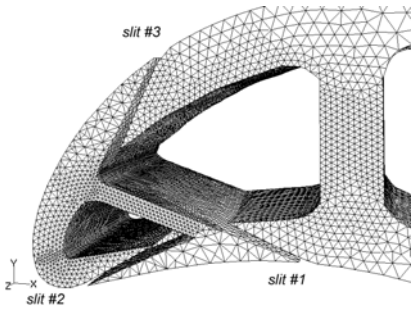

Fig. 16: Computional 3-dimensional grid of the solid part at the leading edge area

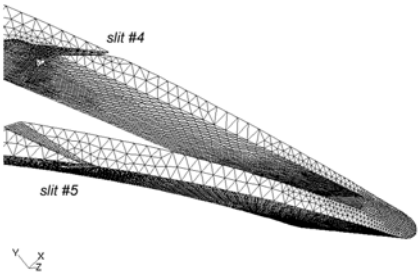

Fig. 17: Computional 3-dimensional grid of the solid part at the trailing edge area

The geometrical dimensions of the 3-dimensional slits is shown in Fig. 18 and is the result of the optimisation through several CFD-calculations and measurements of Jericha et al. (1997), Gehrer et al. (1997), and Moser et al (1998, 1999).

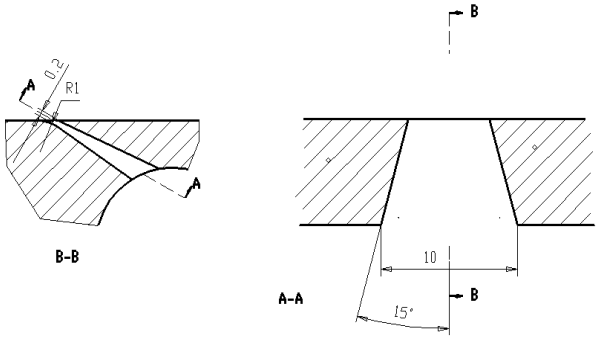

Fig.18: Geometry of the 3-dimensional slit

Results of the 3-Dimensional Flow Analysis

The results of these 3-dimensional CFD-calculations were used as input to the FEA mainly. For that reason the results will be presented in Fig. 19 and 20 as input to the FEA.

FINITE ELEMENT ANALYSIS OF THE TURBINE BLADE

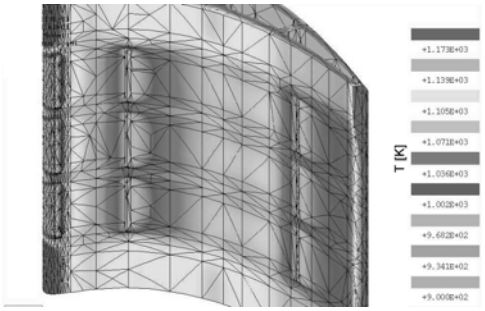

Fig.19: Temperature distribution [K] at pressure side transformed from CFD-solution to FEA-Software Package (”Mechanica”, Parametric Technology Corporation) as input to the FEA.

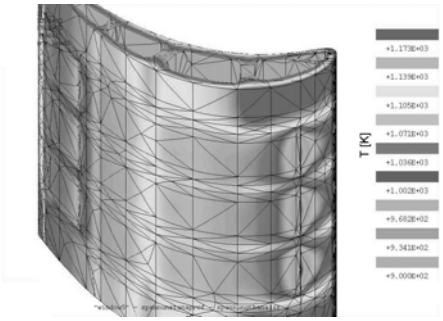

Fig. 20: Temperature distribution [K] at pressure side transformed from CFD-solution to FEA-Software Package as input to the FEA.

For the FEA presented here a p-method had been used (PRO/MECHANICA, PARAMETRICAL TECHNOLOGY CORP.), which is commonly called ”geometrical element method (GEM)”. This method represents the displacement and temperature within each element using high-order polynomials, as opposed to the linear or sometimes quadratic or cubic functiones used in conventional FEA.

Model

With this FEA-software package Pro/MECHANICA we created a numerical model to simulate the stress. In the inner cooling channels we assumed a fixed heat transfer coefficient of 550 W/m^2K and a cooling fluid temperature of 773 K. In the cooling slits, on the pressure and the suction side of the blades we used the heat flux distributions and wall temperatures provided by the 3-dimensional CFD analysis. As additional condition we added a centrifugal force equivalent to 10,500 rpm. The model was fixed at the hub in radial direction. As material we used L326 VMR (Table 6, above).

Results of the Finite Element Analysis

Figs.21 and 22 present the ”von Mises”-stresses. The maximum stress repesented equals 480 N/mm^2. This stress corresponds to the 0.2 creep limit for L326 VMR at 1173 K. In 0.2 creep limit diagram (Fig.23) no point exceeds the 0.2% creep limit. In the creep rapture strength diagram some points exceed the limit. These points are located at the pressure side behind the first slit row, the suction side between the slits and on the trailing edge.

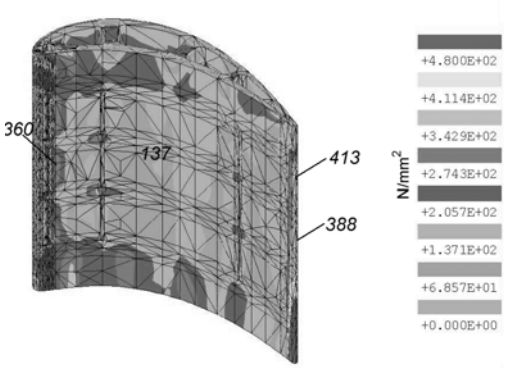

Fig. 21: The stress distribution ”von Mises” at pressure side

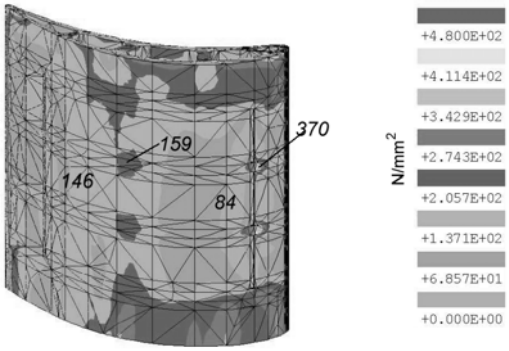

Fig. 22: The stress distribution ”von Mises” at suction side

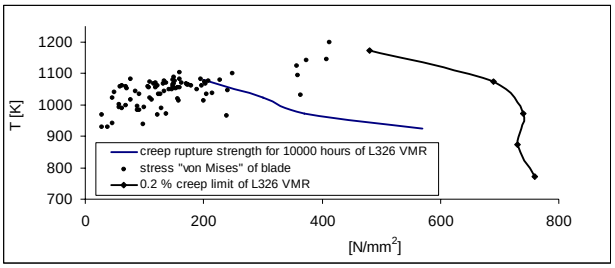

Fig.:23: Creep rupture strength, 0.2 % creep limit of L326 VMR (Alloy 520) and stress distribution of calculated blade at critical points

CONCLUSIONS

The numerical results obtained by CFD and FEA provide a first impression of the advantages and disadvantages of this novel turbine blade cooling.

This type of cooling led to a uniform cooling especially in the area covered by the first slit row (leading edge cooling). In all regions were cooling slits are present we observed a significant decrease in surface temperature. Together with the experimental and numerical results on shock resistance published by Moser et al (1998), this type of cooling provided an optimum coverage of the leading edge area.

In some positions close to the cooling slits we observed high values of stresses caused by large temperature gradients. Here, further optimisation, especially of blade material and slit geometry will be needed.

In this model we did not provide a standard cooling for the trailing edge, since we had been investigating the under expanded cooling films only. The use of this type of standard cooling would certainly be needed to reduce the stresses at the trailing edge.

This model investigation also gave first data on mass flow for each cooling row. As a first estimate we obtained 2.5% MR for each row. Thus it has to be judged carefully which areas have to be covered by under expanded jets and where conventional cooling is sufficient for high temperature and high pressure ratios flows.

From all these considerations we finally come to the conclusion, that starting with two rows of under expanded cooling film coverage – one for the leading edge and one for the pressure side – and conventional cooling for the trailing edge together with superior blade materials we provide an optimum cooling solution for high temperature and high pressure ratio turbine blading.

ACKNOWLEDGEMENT

The authors gratefully acknowledge the support by the Austrian Science Foundation (FWF) under grant P10698 enabling this research on under expanded cooling films.

REFERENCES

Gehrer A., Woisetschläger J., Jericha H., 1997, ”Blade Film Cooling by Under expanded Transonic Jet Layers”, International Gas Turbine & Aeroengine Congress & Exhibition, Orlando, 97

Gilchrist, A. R. and Gregory-Smith, D.G., 1988, ”Compressible Coanda Wall Jet: Predictions of Jet Structure and Comparison with Experiment”, International Journal of Heat and Fluid Flow, Vol.9, pp 286-295

Goldstein Richard J., 1971, ”Film Cooling”, Department of Mechanical Engineering, University of Minnesota, Minneapolis, Minnesota

Gregory-Smith D.G. and Gilchrist A.R., 1987, ”The Compressible Coanda Wall Jet - an Experimental Study of Jet Structure and Breakaway”, Heat and Fluid Flow, Vol. 8, pp 156-164

Gregory-Smith D.G. and Hawkins M., 1991, ”The Development of an Axisymmetric Curved Turbulent Wall Jet”, International Journal of Heat and Fluid Flow, Vol.12, pp 323-330

Ishizuka T., Suzuki A., 1991, ”Steam Injection Aeroderivative Gas Turbine, its Modification Design and Operation Experience”, 19th CIMAC 1991, paper G15

Jericha H., Sanz W., Woisetschläger J., 1997, Oesterreichisches Patent Nr. 406160

Jericha H., Sanz W., Woisetschläger J., Fesharaki M., 1995, ”CO2-Retention Capability of CH4/O2-Fired Graz Cycle”, Proceedings CIMAC 95, paper G07

Moser S, Jericha H., Woisetschläger J, Gehrer A., Reinalter W., 1998, ”The Influence of Pressure Pulses to an innovative Turbine Blade Film Cooling System”, ASME COGEN TURBO POWER ’98

Launder B. E., Spalding D. B., 1972, ”Lectures in Mathematical Models of Turbulence. Academic Press, London, England

Launder B. E., Spalding D. B., 1974, ”The numerical Computation of Turbulent Flows”, Computer Methods in Applied Mechanics and Engineering, 3:269-289.

Moser S., Woisetschläger J, Jericha H., 1999, ”LDA-Untersuchung transsonischer Kühlfilme zur Kühlung moderner Gasturbinenschaufeln”, 7. Fachtagung von ”Lasermethoden in der Strömungsmesstechnik”, Saint-Louis

Satoh T., Watanabe A., Kajita S.,1991, ”Development and Operation of Cheng Cycle Steam Injected Gas Turbine Cogeneration System”, 19th CIMAC 1991, paper G22

Woisetschläger J., Jericha H., Sanz W., Gollner F.,1995, ”Optical Investigation of Transonic Wall-Jet Film Cooling”, ASME COGEN TURBO POWER ’95

Woisetschläger J., Jericha H., Sanz W., Pirker H.P., Seyr A. Ruckenbauer T., 1997, ”Experimental Investigation of Transonic Wall-Jet Film Cooling in a Linear Cascade”, Turbomachinery-Fluid Dynamics and Thermodynamics, Antwerpen, 1997, pp 447-451

Wolfstein M., 1969, ”The Velocity and Temperature Distribution of One-Dimensional Flow with Turbulence Augmentation and Pressure Gradient”, Int. J. Heat Mass Transfer, 12:301-318